Cell Reports

Article

Social isolation impairs the prefrontal-nucleus accumbens circuit subserving social recognition in mice

Graphical abstract

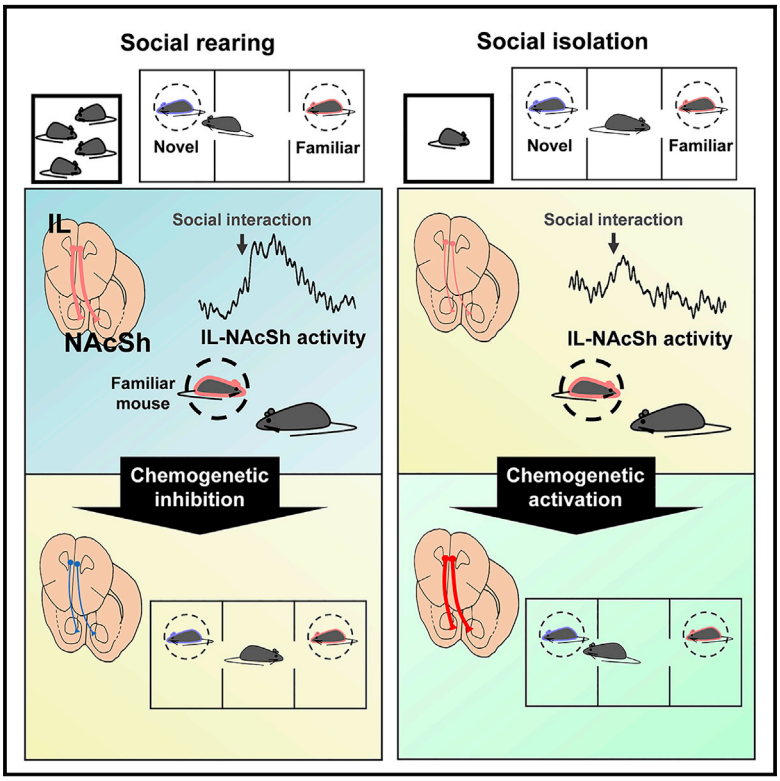

Authors

Gaeun Park, Changhyeon Ryu, Soobin Kim, Se Jin Jeong, Ja Wook Koo, Yong-Seok Lee, Sang Jeong Kim

Correspondence

yongseok7@snu.ac.kr (Y.-S.L.), sangjkim@snu.ac.kr (S.J.K.)

In brief

Park et al. identifies a brain circuit critical for social recognition. Inhibition of the neural projection from infralimbic cortex to nucleus accumbens shell impairs social recognition without affecting social preference, which reconciles the behavioral phenotype shown in socially isolated mice. Reactivation of the same neurons rescues its social recognition deficit.

Highlights

- Social isolation decreases the excitability of NAcSh-projecting IL neurons
- NAcSh-projecting IL neurons are activated by familiar conspecifics
- Inhibition of NAcSh-projecting IL neurons impairs social recognition
- Activating NAcSh-projecting IL neurons rescues social recognition deficit in SH mice

Park et al., 2021, Cell Reports *35*, 109104
May 11, 2021
https://doi.org/10.1016/j.celrep.2021.109104

CellPress

Cell Reports

CellPress
OPEN ACCESS

Article

Social isolation impairs the prefrontal-nucleus accumbens circuit subserving social recognition in mice

Gaeun Park,[1,2,6] Changhyeon Ryu,[1,2,3,6] Soobin Kim,[1,2] Se Jin Jeong,[4] Ja Wook Koo,[4,5] Yong-Seok Lee,[1,2,3,7,*] and Sang Jeong Kim[1,2,3,*]

[1]Department of Physiology, Seoul National University College of Medicine, Seoul 03080, Korea
[2]Department of Biomedical Sciences, Seoul National University College of Medicine, Seoul 03080, Korea
[3]Neuroscience Research Institute, Seoul National University College of Medicine, Seoul 03080, Korea
[4]Emotion, Cognition & Behavior Research Group, Korea Brain Research Institute, Daegu 41062, Korea
[5]Department of Brain and Cognitive Sciences, Daegu Gyeongbuk Institute of Science and Technology (DGIST), Daegu 42988, Korea
[6]These authors contributed equally
[7]Lead contact
*Correspondence: yongseok7@snu.ac.kr (Y.-S.L.), sangjkim@snu.ac.kr (S.J.K.)
https://doi.org/10.1016/j.celrep.2021.109104

SUMMARY

Although medial prefrontal cortex (mPFC) is known to play important roles in social behaviors, how early social experiences affect the mPFC and its subcortical circuit remains unclear. We report that mice singly housed (SH) for 8 weeks after weaning show a social recognition deficit, even after 4 weeks of resocialization. In SH mice, prefrontal infralimbic (IL) neurons projecting to the shell region of nucleus accumbens (NAcSh) show decreased excitability compared with group-housed (GH) mice. NAcSh-projecting IL neurons are activated when GH mice encounter a familiar conspecific, which is not observed in SH mice. Chemogenetic inhibition of NAcSh-projecting IL neurons in normal mice impairs social recognition without affecting social preference, whereas activation of these neurons reverses social recognition deficit in SH mice. Our findings demonstrate that early social experience critically affects mPFC IL-NAcSh projection, the activation of which is required for social recognition by encoding information for social familiarity.

INTRODUCTION

Social behaviors include social preference and social recognition (Albers, 2012; Tanimizu et al., 2017; Young, 2002). Social recognition consists of the behavioral characteristics of distinguishing a novel conspecific from a familiar one, which is evolutionarily well conserved because of its importance for survival (Bicks et al., 2015; Lu et al., 2018; Moy et al., 2004). Social recognition is impaired in several neurodevelopmental disorders, such as autism spectrum disorder (ASD) and schizophrenia (Carter et al., 2011; McKibben et al., 2014; Webb et al., 2010). Although several brain regions, including the hippocampus, have been identified as potential hubs for social recognition, the neural mechanism subserving social recognition remains largely unknown (Deng et al., 2019; Tzakis and Holahan, 2019).

Early social experience is a key environmental factor for postnatal neurodevelopment (Chisholm et al., 1995; Hall, 1998; Weiss et al., 2004), and social deprivation during the critical developmental period has long-lasting effects on social function in adults (Kreppner et al., 1999; Makinodan et al., 2012; Rutter et al., 1999, 2007). Juvenile social isolation (jSI) is one of the animal models widely used to study the effects of early social experiences on postnatal developments and social functions in adulthood. In mice, jSI was shown to result in social behavior deficits in adulthood; however, previous studies using the jSI model mostly focused on its effect on social preference (Bicks et al., 2020; Yamamuro et al., 2020), and the aspects of social behaviors that are more sensitive to jSI have not been fully investigated. In addition, whether the selective deficits, if there are any, can be reversed by resocialization remains controversial (Chugani et al., 2001; Eluvathingal et al., 2006; Liu et al., 2012; Makinodan et al., 2017).

The medial prefrontal cortex (mPFC) is critically involved in social behaviors in both humans and rodents. Imaging studies in humans and mice showed that the mPFC is activated in response to social behaviors (Dang et al., 2019; Fukuda et al., 2019; Kim et al., 2015; Wagner et al., 2016). Optogenetic manipulation of excitation/inhibition balance in the mPFC impairs social interaction in mice (Yizhar et al., 2011). Importantly, the mPFC is one of the brain regions affected by jSI (Fuster, 2002; Layden et al., 2017; Liu et al., 2012; Makinodan et al., 2012; Yamamuro et al., 2020). Early social isolation affects brain structures and physiology, as well as social behaviors (Liu et al., 2012; Medendorp et al., 2018). Recent studies have begun to reveal the mPFC-subcortical circuits that are affected by jSI. For example, Yamamuro and colleagues showed that mPFC

neurons projecting to the posterior paraventricular thalamus (pPVT) are activated by social contacts and that its activities are reduced in jSI mice (Yamamuro et al., 2020). However, whether the mPFC neurons projecting to the other subcortical regions implicated in social behavior, such as the nucleus accumbens (NAc), are affected by jSI remains unknown.

In this study, we examined the impacts of jSI on both social preference and recognition and found that social recognition was severely impaired by jSI, which was not recovered by a prolonged resocialization. The converging evidence presented herein supports the conclusion that a subset of mPFC infralimbic neurons projecting to the shell region of nucleus accumbens (NAcSh), of which excitability is reduced in jSI mice, is critically involved in social recognition by encoding neural information for social familiarity.

RESULTS

Single-housed mice showed deficits in social recognition after resocialization

A previous study showed that resocialization for 4 weeks was sufficient to restore impairments in social interaction induced by 8 weeks of social isolation (Liu et al., 2012). We examined whether other social phenotypes are also affected by an isolation-regrouping protocol (Figure 1A). We used the three-chamber test to test social preference and recognition (Moy et al., 2004; Figure 1B). In the social preference test, SH mice spent significantly more time exploring a conspecific than an object, showing that the social preference is at least partially restored in SH mice after resocialization (Figures 1C, S1D, and S1F). However, SH mice did not spend significantly more time interacting with novel conspecifics compared with familiar conspecifics, whereas GH mice spent significantly more time interacting with novel conspecifics, suggesting that SH mice have a severe deficit in social recognition (Figures 1D, S1E, and S1G). SH mice showed performance comparable to that of GH mice in the novel object recognition test, demonstrating that SH mice do not have a deficit in general recognition memory (Figure 1E). Furthermore, the object place recognition test was performed to examine whether SH mice have a deficit in hippocampus-dependent memory (Squire and Zola-Morgan, 1991; Figure 1F). Again, SH mice investigated an object in a novel position significantly more than an object in a familiar position, demonstrating that SH mice do not have a hippocampus-dependent memory deficit. GH and SH mice showed comparable body-mass changes (Figure S1A). In addition, SH and GH mice showed comparable basal locomotor activity and anxiety levels (Figures S1B and S1C).

We also tested the effects of different durations of social isolation and resocialization on social behaviors. When mice were housed alone for 2 weeks immediately after weaning—the critical period for the development of the mPFC—and introduced back into a group for 4 weeks, SH mice showed performance to that of comparable GH mice in both social preference and recognition tests (Figures S2A–S2D). We also tested whether regrouping SH mice for longer than 4 weeks may rescue the impaired social recognition ability in SH mice (Figure S2E). Interestingly, SH mice still showed a deficit in social recognition, but not in social preference, at 8 weeks following regrouping (Figures S2F–S2H).

Single-housed mice showed reduced NAcSh-projecting IL neuronal excitability

Previous studies showed that the hippocampus plays a critical role in social recognition (Hitti and Siegelbaum, 2014; Okuyama et al., 2016). In particular, the connection between the ventral hippocampus CA1 and the NAcSh was shown to be important for distinguishing a novel conspecific (Okuyama et al., 2016). Because the mPFC regulates social behavior via its connection to subcortical regions, including the NAcSh, which is also implicated in social behaviors (Kohls et al., 2013; Krishnan et al., 2007; Loureiro et al., 2019), we hypothesized that the neural projection from the mPFC to the NAcSh might be involved in social recognition. Neurons in the ventral mPFC regions, including the deep layer of the infralimbic (IL) cortex, were heavily labeled by retrograde enhanced green fluorescent protein (EGFP) virus injection into the NAcSh (Figures 2A, 2B, S3A, and S4A). Although the neuronal projection from the prelimbic (PL) cortex to the NAcSh was also labeled, the density of this tract was diminished relative to that spanning the IL and NAcSh, which was consistent with a previous report (Murugan et al., 2017; Figure 2B). Whole-cell patch-clamp recordings of *ex vivo* brain slices revealed that NAcSh-projecting IL neurons in the deep layer exhibited significantly reduced neuronal excitability in SH mice compared with in GH mice (Figure 2C). Reduced neuronal excitability was not observed in NAcSh-projecting PL neurons (Figure 2D). Moreover, NAcSh-projecting IL neurons (EGFP positive) showed decreased excitability compared with tentative non-NAcSh-projecting IL neurons (EGFP negative) in SH mice (Figure S4B), suggesting that the impact of single housing on neuronal excitability is target specific and limited to neural subregions. In GH mice, EGFP-positive and EGFP-negative neurons showed comparable excitability (Figure S4B). The input resistance of NAcSh-projecting IL neurons in SH mice was also significantly lower than in GH mice (Figure S4E), which is consistent with the aforementioned reduced excitability. Other electrophysiological properties, including excitatory synaptic transmission, were not different between GH and SH mice (Figure S4).

NAcSh-projecting IL neurons are activated by a familiar conspecific

To confirm the social recognition deficit in SH mice in a different behavioral paradigm, we used social habituation/recognition tasks (Figure 3A). During the habituation session, mice were consecutively exposed to the same target mouse. Both GH and SH mice showed significantly decreased interaction time with the conspecifics in the habituation session (Figure 3B). In the social recognition session, which was performed on the following day, mice were allowed to explore an empty cup, a novel conspecific, or a familiar conspecific. GH mice showed a significant preference toward the novel mouse over either the empty cup or the familiar mouse (Figure 3C). However, SH mice spent a comparable amount of time exploring the novel and familiar conspecifics (Figure 3C), suggesting that SH mice show impaired social recognition.

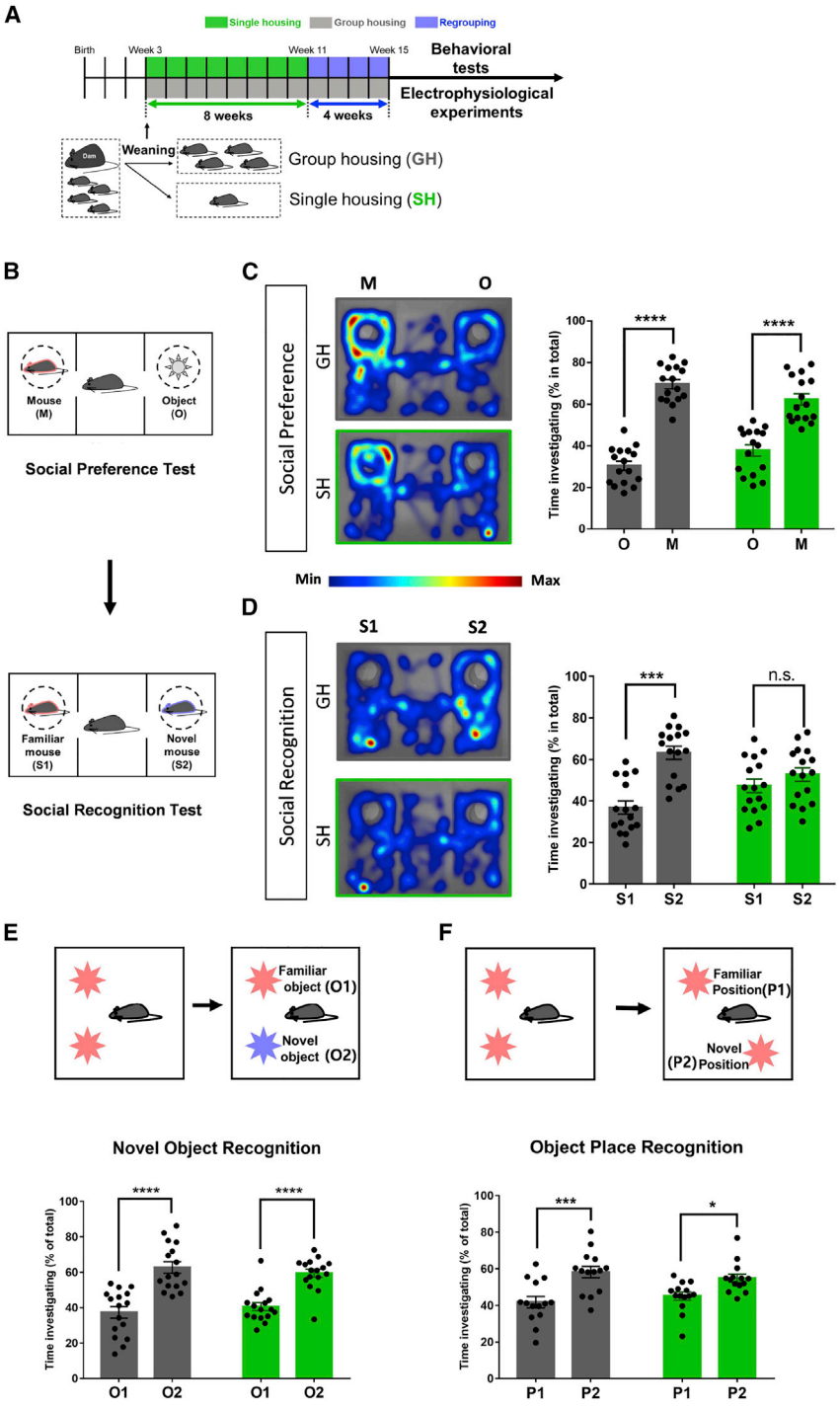

Figure 1. Juvenile social isolation impairs social recognition in adulthood, even after resocialization

(A) Timeline of the social isolation model used in this study. Single-housed (SH) mice are singly housed for 8 weeks and regrouped for at least 4 weeks before tests. Group-housed (GH) mice were used as the control group.

(B) Schematic for three-chamber social behavior tests. M, target conspecific; O, inanimate object; S1, familiar conspecific; S2, novel conspecific.

(C) Left: representative heatmap images of social behavior during the social preference test. Right: in the social preference test, both GH and SH mice spent significantly more time exploring a target conspecific than an inanimate object in the resocialization period. Two-way ANOVA: GH, n = 16 mice; SH, n = 16 mice; interaction between housing and target, $F_{1,60} = 8.904$, $p = 0.0041$. Sidak's multiple comparison test: GH, mouse versus object $t_{60} = 11.21$, ****$p < 0.0001$; SH, mouse versus object $t_{60} = 6.989$, ****$p < 0.0001$.

(D) Left: representative heatmap image of social behavior during the social recognition test. Right: in the social recognition test, SH mice did not show a significant preference toward a novel conspecific versus a familiar conspecific, whereas GH mice shows a significant preference for novel conspecifics. Two-way ANOVA: GH, n = 16 mice; SH, n = 16 mice; interaction between housing and social target, $F_{1,60} = 10.59$, $p = 0.0019$. Sidak's multiple comparison test: GH, S1 versus S2 $t_{60} = 5.811$, ****$p < 0.0001$; SH, S1 versus S2 $t_{60} = 1.208$, $p = 0.4101$. n.s., not significant.

(E) Top: schematic for novel object recognition test. O1, familiar object; O2, novel object. Bottom: both SH mice and GH mice spent significantly more time investigating the novel object than the familiar object. Two-way ANOVA: GH, n = 16 mice; SH, n = 16 mice; interaction between housing and object, $F_{1,60} = 1.341$, $p = 0.2515$. Sidak's multiple comparison test: GH, familiar object versus novel object $t_{60} = 6.343$, ****$p < 0.0001$; SH, familiar object versus novel object $t_{60} = 4.705$, ****$p < 0.0001$.

(F) Top: schematic for the object place recognition test. P1, familiar position; P2, novel position. Bottom: both SH mice and GH mice spent significantly more time investigating an object in a novel position than the object in a familiar position. Two-way ANOVA: GH, n = 14 mice; SH, n = 14 mice; interaction between housing and position, $F_{1,52} = 1.482$, $p = 0.2290$. Sidak's multiple comparison test: GH, object in familiar position versus object in novel position $t_{52} = 4.287$, $p = 0.0002$; SH, object in familiar position versus object in novel position $t_{52} = 2.565$, *$p = 0.0263$.

Because the subject mice were exposed to either a familiar or a novel mouse in this behavioral paradigm, we could examine whether the NAcSh-projecting IL neurons are differentially activated by distinct social stimuli (familiar versus novel conspecific) by monitoring the neuronal activity using c-Fos immunohistochemistry after the social recognition session (Figure 3D). To monitor the neuronal activity selectively in the NAcSh-projecting IL neurons after social interaction with either a familiar or a novel mouse, we injected a retrograde adeno-associated virus (AAVrg) encoding the enhanced green fluorescent protein (EGFP) into the NAcSh in both SH and GH mice (Figure 3D). When we analyzed c-Fos and EGFP co-labeled neurons in the IL after the mice were exposed to either a novel or a familiar conspecific (Figure 3E), the GH mice that interacted with a familiar conspecific showed

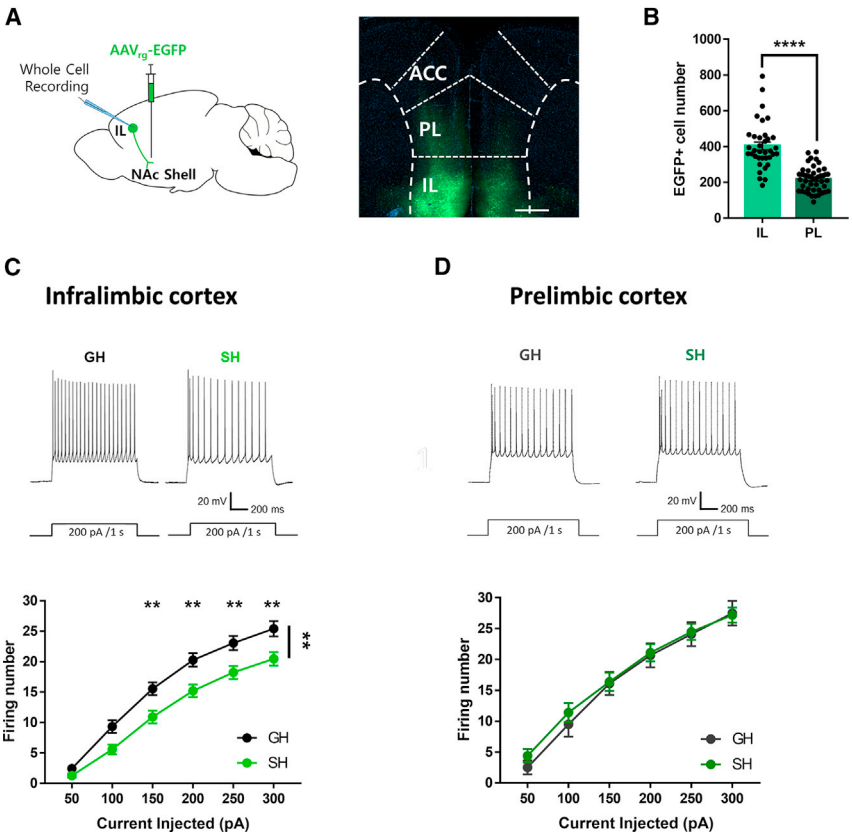

Figure 2. Excitability of NAcSh-projecting IL neurons is decreased in SH mice

(A) Left: strategy of labeling IL neurons targeting the shell region of nucleus accumbens (NAcSh) by injecting a retrograde adeno-associated virus (AAVrg) expressing EGFP into the NAcSh. Right: representative image showing EGFP expression in the prefrontal cortex. Scale bar, 500 μm.

(B) Quantification of EGFP-labeled cells in the infralimbic (IL) and prelimbic (PL) cortices. IL, n = 47 slices from 16 mice; PL, n = 36 slices from 15 mice. Two-tailed unpaired t test, ****$p < 0.0001$.

(C) Top: representative traces of whole-cell patch-clamp recording in NAcSh-projecting IL neurons. Step currents (200 pA, 1 s) were administered. Bottom: summary data of the number of action potentials evoked in response to 300 pA currents steps. The number of spikes was significantly decreased in the IL→ NAcSh neurons of SH mice relative to those of GH mice. Two-way ANOVA with repeated measures: GH, n = 37 cells from 14 mice; SH, n = 55 cells from 14 mice; interaction between housing and injected current, $F_{5,450} = 3.334$, $p = 0.0057$; effect of housing, $F_{1,90} = 11.16$, $p = 0.0012$. Sidak's multiple comparison test: 150 pA, **$p = 0.0075$; 200 pA, **$p = 0.0025$; 250 pA, **$p = 0.0045$; 300 pA, **$p = 0.0035$.

(D) Top: representative traces of whole-cell patch-clamp recording in NAcSh-projecting PL neurons. Bottom: summary data of the number of action potentials evoked in response to 300 pA currents steps. NAcSh-projecting PL neurons in SH and GH mice showed comparable excitability. Two-way ANOVA with repeated measures: GH, n = 12 cells from 6 mice; SH, n = 21 cells from 5 mice; interaction between housing and injected current, $F_{5,155} = 0.7222$, $p = 0.6077$; effect of housing, $F_{1,31} = 0.1391$, $p = 0.7117$. Sidak's multiple comparison test: 50 pA, $p = 0.9565$; 100 pA, $p = 0.9565$; 150–300 pA, $p > 0.9999$.

significantly more co-labeled neurons in the IL than did the GH mice that interacted with neither an empty cup nor the novel conspecific (Figure 3F). The SH mice did not show conspecific-induced c-Fos activation in the IL (Figure 3F). This significant increase in the number of c-Fos/EGFP co-labeled neurons was not observed in the PL of either GH or SH mice; however, GH mice showed a strong trend toward increased c-Fos expression, regardless of the familiarity of the target mice (Figure 3G). We also counted the number of total c-Fos-positive cells without considering EGFP expression (Figure S5). In the IL cortex, the numbers of total c-Fos-positive cells were comparable between the groups (Figure S5A). However, as previously reported (Kim et al., 2015; Numa et al., 2019), significantly more c-Fos-positive cells were observed in the PL of the GH mice that interacted with either familiar or novel conspecifics compared with the GH mice that interacted with the empty cup (Figure S5B). Altogether, our results suggest that the NAcSh-projecting IL neurons are specifically activated by familiar conspecifics.

Next, we performed *in vivo* Ca^{2+} imaging using fiber photometry to confirm the familiar mouse-induced activation of the NAcSh-projecting IL neurons by expressing a genetically encoded fluorescent Ca^{2+} indicator (GCaMP6s) in the NAcSh-projecting IL neurons (Figures 4A and 4B). The social habituation/recognition task was used, and the Ca^{2+} signal was monitored in the IL cortex during the recognition session (Figure 4C). Consistent with the c-Fos immunohistochemistry data, NAcSh-projecting IL neurons in GH mice showed a robust increase in Ca^{2+} signal when they interacted with a familiar conspecific, whereas these neurons did not respond to a novel conspecific (Figures 4D, 4E, and S6). The NAcSh-projecting IL neurons in SH mice did not show this familiar conspecific-induced neuronal activation (Figures 4F, 4G, and S6). Altogether, these results show that NAcSh-projecting IL neurons are activated as a consequence of interacting with familiar conspecifics.

IL-NAcSh circuit is required for social recognition

To determine whether the NAcSh-projecting IL neurons are critically involved in social recognition, we chemogenetically inhibited these neurons in normal GH mice (Figure 5A). The hM4Di receptor is specifically expressed in the NAcSh-projecting IL neurons (Figures 5B and S3B). hM4Di or control virus (mCherry)-expressing mice were intraperitoneally (i.p.) injected with clozapine-N-oxide (CNO), which was confirmed to reduce neuronal excitability in hM4Di-expressing neurons (Figures 5C and 5D). Behavior tests were performed 40 min after the CNO or vehicle injection. Inhibition of the NAcSh-projecting IL neurons did not affect the social preferences of the mice (Figures 5E, S7A, and S7C). When these neurons were inhibited, mice spent less time investigating novel mice and had a decreased preference index for social recognition compared with the vehicle-injected

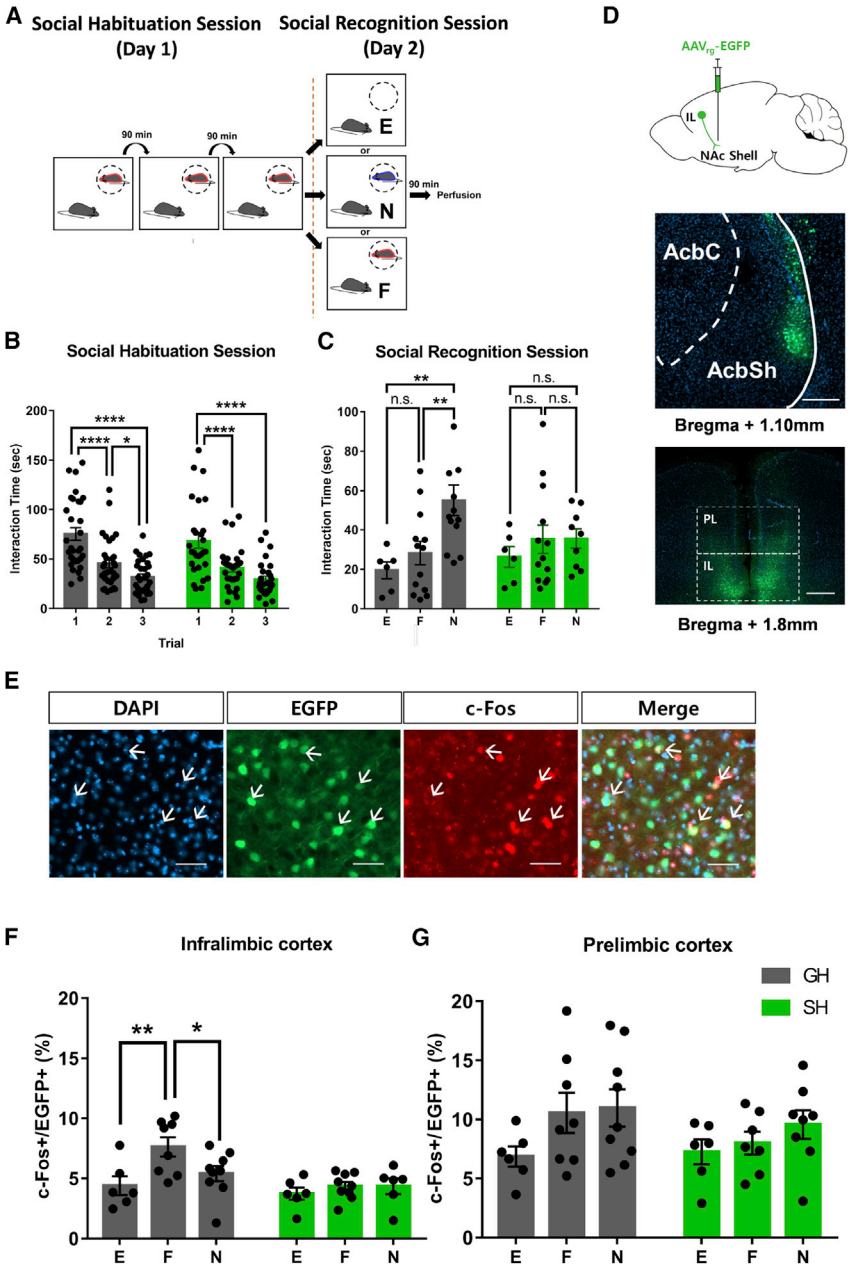

Figure 3. NAcSh-projecting IL neurons are activated by encountering a familiar mouse

(A) Experimental scheme for the social habituation/social recognition task. Habituation session: GH or SH mice were exposed to the same conspecifics three times for 5 min with a 90-min interval. Social recognition session: mice were exposed to familiar conspecifics, novel conspecifics, or an empty cup. E, empty cup; F, familiar target conspecific; N, novel target conspecific.

(B) Both GH and SH mice show significantly decreased interaction times during the social habituation session. Two-way ANOVA with repeated measures: GH, n = 31 mice; SH, n = 28 mice; interaction between housing and trial, $F_{2,114}$ = 0.1866, p = 0.8300. Tukey's multiple comparison test: GH, 1 versus 2 t_{31} = 5.438, ****p < 0.0001; GH, 1 versus 3 t_{31} = 7.983, ****p < 0.0001; GH, 2 versus 3 t_{31} = 2.545, *p = 0.0364; SH, 1 versus 2 t_{28} = 4.723, ****p < 0.0001; SH, 1 versus 3 t_{28} = 6.744, ****p < 0.0001; SH, 2 versus 3 t_{28} = 2.01, p = 0.1339.

(C) SH mice failed to discriminate familiar conspecifics from novel conspecifics. GH mice showed significantly longer interaction times with novel conspecifics than with familiar conspecifics. Two-way ANOVA: n = 6 mice (GH, E), n = 13 mice (GH, F), n = 13 mice (GH, N); n = 6 mice (SH, E), n = 13 mice (SH, F), n = 9 mice (SH, N); interaction between housing and target, $F_{2,54}$ = 2.461, p = 0.0948. Tukey's multiple comparison test: GH, E versus F t_{54} = 1.158, p = 0.6929; GH, E versus N t_{54} = 4.655, **p = 0.0049; GH, F versus N t_{54} = 4.4, **p = 0.0082; SH, E versus F t_{54} = 1.169, p = 0.6881; SH, E versus N t_{54} = 1.142, p = 0.7000; SH, F versus N t_{54} = 0.05694, p = 0.9991.

(D) Top: strategy for labeling NAcSh-projecting IL neurons. The retrograde fluorescence virus (AAVrg-EGFP) was injected into the NAcSh. Middle: representative image of the brain slices of NAcSh where the virus was injected. Scale bar, 200 μm. Bottom: representative image of mPFC expressing retrogradely transported EGFP virus. Scale bar, 500 μm.

(E) Representative images showing fluorescence for NAcSh-projecting IL neurons labeled with EGFP (green), c-Fos (red), and DAPI (blue) and the merged image. White arrows indicate co-labeled cells for EGFP and c-Fos. Scale bar, 20 μm.

(F) GH mice show significantly increased numbers of c-Fos-positive NAcSh-projecting IL neurons when they encountered familiar conspecifics. However, SH mice showed no difference in the number of activated neurons depending on the familiarity of the target mice. Two-way ANOVA: n = 6 mice (GH, E), n = 8 mice (GH, F), n = 9 mice (GH, N); n = 6 mice (SH, E), n = 9 mice (SH, F), n = 6 mice (SH, N); interaction between housing and target, $F_{2,38}$ = 2.553, p = 0.0911. Tukey's multiple comparison test: GH, E versus F t_{38} = 4.92, **p = 0.0036; GH, E versus N t_{38} = 1.574, p = 0.5119; GH, F versus N t_{38} = 3.76, *p = 0.0300; SH, E versus F q_{38} = 0.9601, p = 0.7771; SH, E versus N t_{38} = 0.8705, p = 0.8125; SH, F versus N t_{38} = 0.006479, p > 0.9999.

(G) GH mice shows increased numbers of c-Fos-positive NAcSh-projecting PL neurons when they encountered either familiar or novel conspecifics. Two-way ANOVA: n = 6 mice (GH, E), n = 8 mice (GH, F), n = 9 mice (GH, N); n = 6 mice (SH, E), n = 9 mice (SH, F), n = 6 mice (SH, N); interaction between housing and target, $F_{2,38}$ = 0.5333, p = 0.5910. Tukey's multiple comparison test: GH, E versus F t_{38} = 2.615, p = 0.1676; GH, E versus N t_{38} = 2.982, p = 0.1015; GH, F versus N t_{38} = 0.3279, p = 0.9708; SH, E versus F t_{38} = 0.5079, p = 0.9315; SH, E versus N t_{38} = 1.635, p = 0.4861; SH, F versus N t_{38} = 1.161, p = 0.6927.

mice (Figures 5F, S7B, and S7D). CNO injection did not affect social preference or recognition in control virus-expressing mice (Figures 5E and 5F). These results demonstrate that NAcSh-projecting IL neuronal activity is required for normal social recognition. Importantly, inhibiting NAcSh-projecting IL neurons did not affect the novel object recognition or object place recognition test (Figures S8A and S8B). In addition, inhibiting this neuronal activity did not affect basal locomotor activity or anxiety levels (Figures S8C–S8E). The forced swim test (FST) was also performed to test whether manipulating this neuronal activity causes depressive-like behavior (Porsolt et al., 1977). However, inactivating NAcSh-projecting IL neurons did not affect the

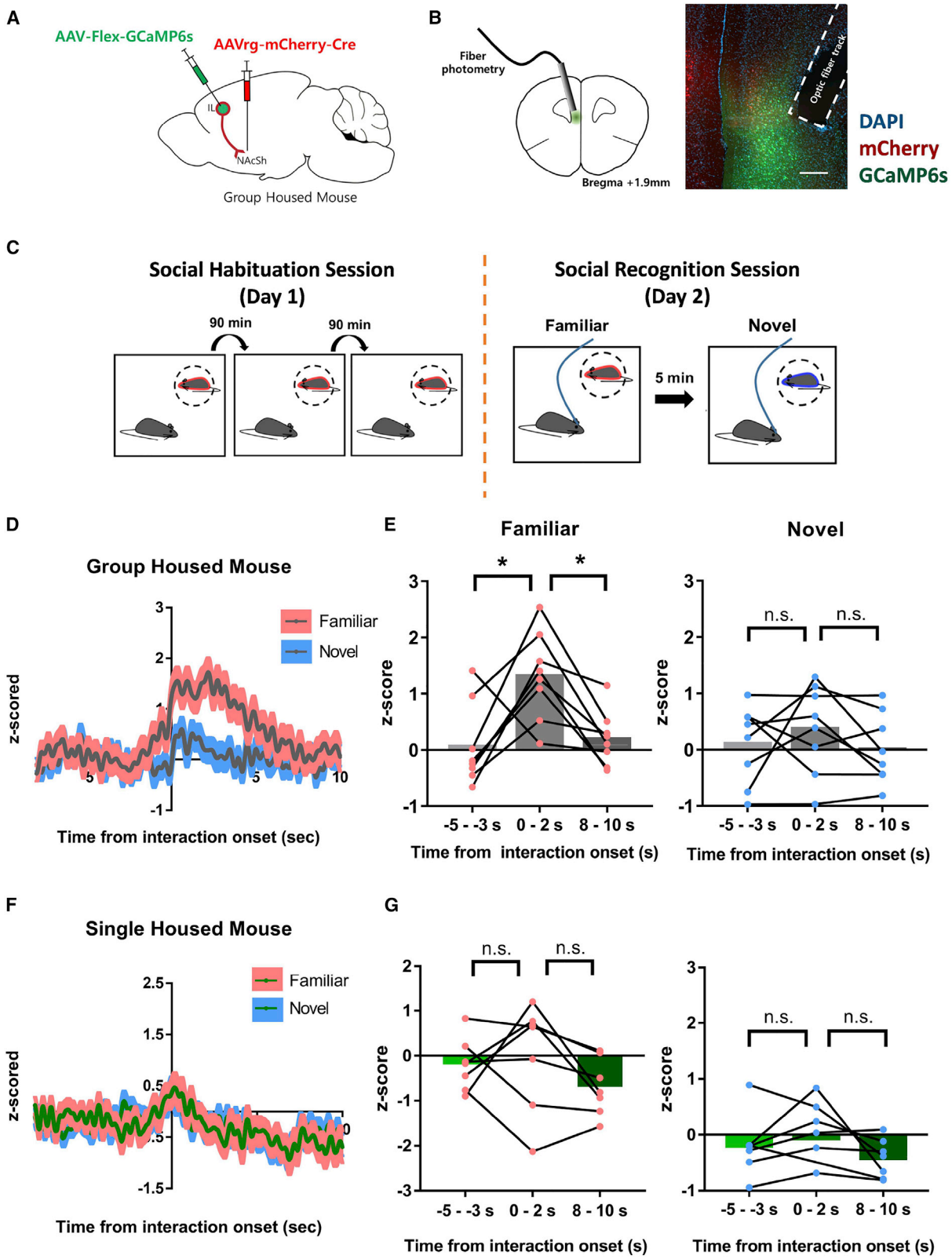

(legend on next page)

immobility time in the FST (Figure S8F). We also found that the normal GH mice did not distinguish a novel mouse from its cage mate when the NAcSh-projecting IL neurons were inhibited (Figures S7F and S7G). However, this manipulation did not affect the reciprocal social interaction with a novel conspecific, showing that this neuronal activity is less likely to affect sociability (Figure S7E). Altogether, our results strongly suggest that the NAcSh-projecting IL neurons may encode social familiarity and contribute to social recognition.

We also examined whether the NAcSh-projecting PL neurons are involved in social behaviors by expressing the hM4Di receptor specifically expressed in the NAcSh-projecting PL neurons (Figures S9A–S9C). Although CNO injection did not affect the total exploration time in the social preference or recognition sessions (Figures S9D and S9E), inhibiting the NAcSh-projecting PL neurons had mild but significant effects on both social preference and recognition (Figures S9F–S9I). CNO-injected mice showed significantly reduced preference indices but still demonstrated a significant preference for a mouse over an object and a novel mouse over a familiar mouse in the social preference and recognition tests, respectively (Figures S9F–S9I). These results demonstrate that the PL-NAcSh circuit is involved in both social recognition and preference in mice.

Increasing NAcSh-projecting IL neuronal activity rescues the social recognition deficit in SH mice

We examined whether increasing NAcSh-projecting IL neuronal activity could rescue the social recognition deficit in SH mice. To selectively activate these neurons, we expressed the hM3Dq receptor in NAcSh-projecting IL neurons and injected CNO (1 mg/kg, i.p.) 40 min before behavioral tests (Figures 6A–6D). We compared the social behaviors of the CNO-injected SH mice with those of the vehicle-injected SH mice. Although the SH mice spent more time exploring the mouse than the object in the social preference test regardless of CNO treatment (Figures 6E, S10A, and S10C), the vehicle-injected SH mice showed a deficit in the social recognition test (Figure 6F). The CNO-injected SH mice spent significantly more time exploring the novel mouse than the familiar mouse, demonstrating that the social recognition deficit in SH mice can be rescued by enhancing the activity of NAc-projecting IL neurons (Figures 6F, S10B, and S10D). CNO injection, even at a higher dose (3 mg/kg), did not affect social behaviors in mCherry-expressing mice (Figures 5E and 5F). In addition, CNO injection did not affect social behaviors in the hM3Dq-receptor-expressing GH mice (Figure S11).

DISCUSSION

In this study, we found that a subpopulation of mPFC IL neurons projecting to the NAcSh is activated by a familiar conspecific and that its inactivation impairs social recognition in normal mice. These results suggest that the IL-NAcSh circuit encodes social familiarity. We also showed that the excitability of the NAcSh-projecting IL neurons is decreased in jSI mice, which may underlie the social recognition deficit caused by jSI.

Social memory/recognition is governed by several brain regions, including the hippocampus (Hitti and Siegelbaum, 2014; Meira et al., 2018; Okuyama et al., 2016; Piskorowski et al., 2016). Among the different hippocampal subregions, the dorsal CA2 (dCA2) has been shown to be critically involved in social memory in so far as it detects social novelty (Donegan et al., 2020; Hitti and Siegelbaum, 2014). The dCA2 neurons project to the ventral CA1 (vCA1), which encodes social engrams (Meira et al., 2018; Okuyama et al., 2016). The vCA1 social engram neurons send their projections to the NAcSh, the activation of which is required for social memory (Okuyama et al., 2016). In addition to this dCA2-vCA1-NAcSh circuit, we found that the mPFC IL-NAcSh circuit is involved in processing social memory. Interestingly, the vCA1 neurons provide direct inputs to the mPFC, which is more robust in the IL than the PL (Liu and Carter, 2018; Wang et al., 2018). Therefore, although further studies are required, it is conceivable that neuronal inputs from vCA1 social engram cells drive the activity of NAcSh-projecting IL neurons, which in turn project to the NAcSh, a brain region that translates motivation

Figure 4. NAcSh-projecting IL neurons are activated by a familiar conspecific *in vivo*

(A) Strategy of expressing a genetically encoded calcium indicator (GCaMP6s) specifically in NAcSh-projecting IL neurons by injecting a Cre-dependent GCaMP6s virus (Flex-GCaMP6s) in the IL and retrograde mCherry-Cre virus in the NAcSh of GH or SH mice.

(B) Diagram and representative image showing GCaMP6s expression and optic cannula track in IL. Scale bar, 500 μm.

(C) Experimental scheme for Ca^{2+} activity recording of NAcSh-projecting IL neurons during social behavior by using fiber photometry. Ca^{2+} activity was monitored during the social recognition session.

(D) GCaMP6s signals of NAcSh-projecting IL neurons in GH mice showed an increased mean z-score when the mice interacted with a familiar conspecific (red), but not with a novel conspecific (blue). n = 8 mice (GH).

(E) Left: mean GCaMP6s signals of NAcSh-projecting IL neurons in a GH mouse increased significantly 0–2 s after the onset of interactions with familiar mice. One-way ANOVA with repeated measures: GH, n = 8 mice; $F_{1.68,11.76} = 7.71$, p = 0.0092. Tukey's multiple comparison tests: −5 to ~−3 s versus 0 to ~2 s $t_7 = 4.317$, *p = 0.0432; −5 to ~−3 s versus 8 to ~10 s $t_7 = 0.537$, p = 0.9244; 0 to ~2 s versus 8 to ~10 s $t_7 = 5.75$, *p = 0.0116. Right: significant increase in GCaMP6s signal by interaction onset was not observed during interaction with novel conspecifics. One-way ANOVA with repeated measures: GH, n = 8 mice; $F_{1.409,9.862} = 1.065$, p = 0.3552. Tukey's multiple comparison tests: −5 to ~−3 s versus 0 to ~2 s $t_7 = 1.15$, p = 0.7072; −5 to ~−3 s versus 8 to ~10 s $t_7 = 0.6125$, p = 0.9032; 0 to ~2 s versus 8 to ~10 s $t_7 = 2.45$, p = 0.2595.

(F) GCaMP6s signals of NAcSh-projecting IL neurons in SH mice did not show increased mean z-score when the mice interacted with either a familiar conspecific (red) or a novel conspecific (blue). n = 7 mice (SH).

(G) Left: mean GCaMP6s signals of NAcSh-projecting IL neurons in SH mice did not significantly change 0–2 s after the onset of interaction with familiar mice. One-way ANOVA with repeated measures: SH, n = 7 mice; $F_{1.258,7.548} = 1.882$, p = 0.2139. Tukey's multiple comparison tests: −5 to ~−3 s versus 0 to ~2 s $t_6 = 0.5636$, p = 0.9173; −5 to ~−3 s versus 8 to ~10 s $t_6 = 2.903$, p = 0.1805; 0 to ~2 s versus 8 to ~10 s $t_6 = 2.917$, p = 0.1783. Right: GCaMP6s signal in NAcSh-projecting IL neurons in SH mice was not significantly changed by interaction with novel conspecifics. One-way ANOVA with repeated measures: SH, n = 7 mice; $F_{1.971,11.83} = 1.138$, p = 0.3523. Tukey's multiple comparison tests: −5 to ~−3 s versus 0 to ~2 s $t_6 = 0.7476$, p = 0.8606; −5 to ~−3 s versus 8 to ~10 s $t_6 = 0.1.423$, p = 0.6001; 0 to ~2 s versus 8 to ~10 s $t_6 = 2.062$, p = 0.3732.

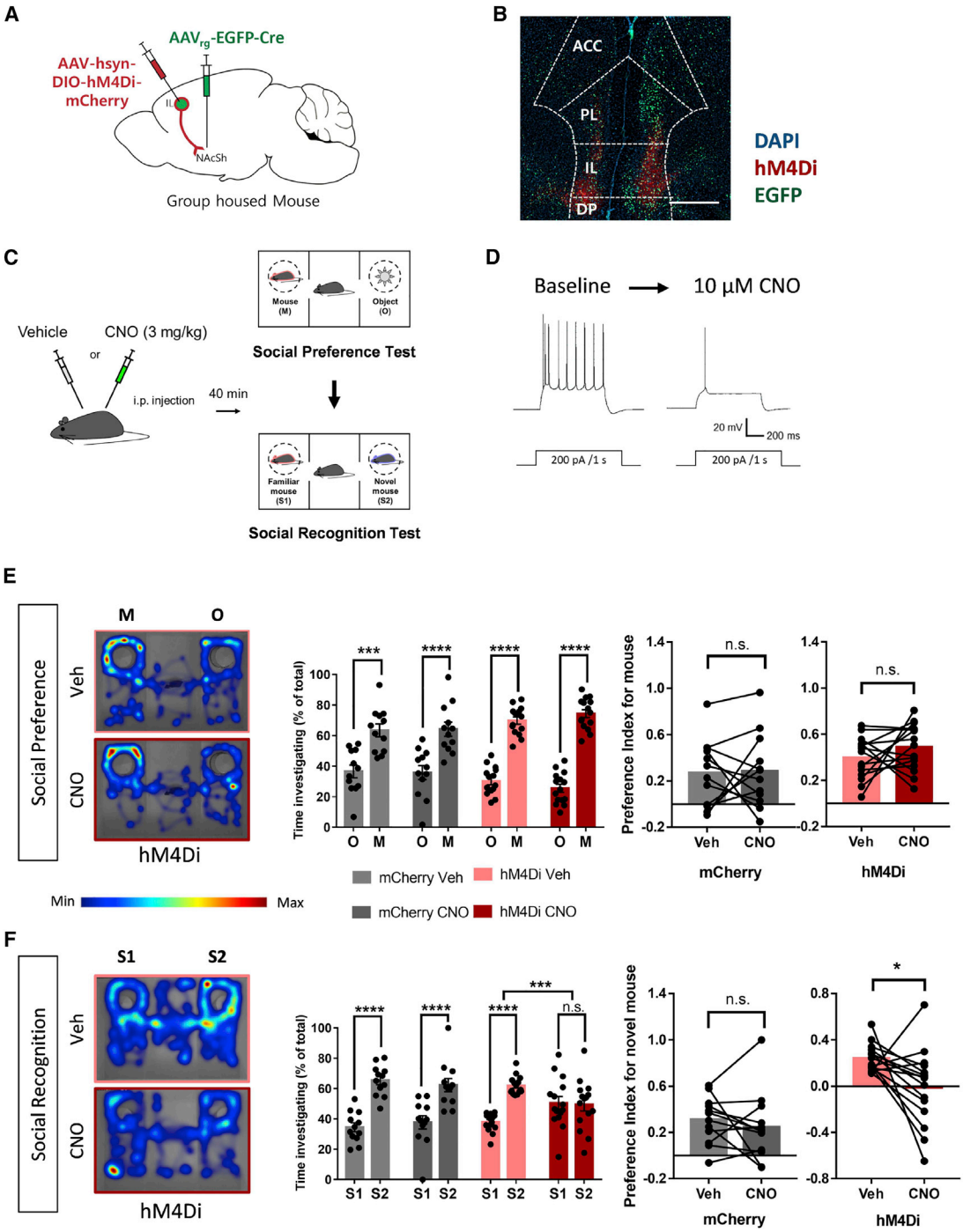

Figure 5. Chemogenetic inactivation of IL-NAcSh neurons selectively impairs social recognition

(A) Strategy of specifically expressing inhibitory G-protein (Gi)-coupled hM4Di receptor or mCherry in NAcSh-projecting IL neurons by injecting a Cre-dependent hM4Di or mCherry virus in the IL and retrograde EGFP-Cre virus in the NAcSh of mice without social isolation.

(B) Representative image of mPFC expressing hM4Di protein preferentially in IL neurons. Scale bar, 500 μm.

(C) Experimental scheme for inhibiting hM4Di-expressing IL→NAcSh neurons. Mice were injected with either 3 mg/kg of clozapine-N-oxide (CNO) or vehicle (saline) and subjected to the 3-chamber social behavior tests.

(D) Representative traces of slice whole-cell patch-clamp recordings that confirmed the inhibitory effect of CNO in a hM4Di neuron.

(E) Left: representative heatmap image of CNO- and vehicle-injected hM4Di-expressing mice subjected to the social preference test. Middle: inactivation of the IL-NAcSh neurons did not affect social preference. Two-way ANOVA with repeated measures: mCherry group, n = 12 mice; interaction between treatment and target, $F_{1,22} = 0.0422$, p = 0.8391. Sidak's multiple comparison test: mCherry Veh, mouse versus object $t_{44} = 4.335$, ***p = 0.0002; mCherry CNO, mouse versus

(legend continued on next page)

into action (Klawonn and Malenka, 2018). How the activation of the IL-NAcSh or the vCA1-NAcSh circuit prompts mice to preferentially approach novel conspecifics rather than familiar conspecifics also requires further investigation. Identifying the cell types of the NAcSh recipient neurons and their downstream targets might be insightful.

The importance of the IL-NAcSh circuit was initially demonstrated in relation to drug-seeking behaviors and addictions. Because the nucleus accumbens is a key node for the mesolimbic dopaminergic pathway, neuronal projection toward the NAcSh was studied in the context of the reward and motivation system (Corbit et al., 2001; Lafferty et al., 2020; Lee et al., 2016; Li et al., 2018). However, the mesolimbic dopaminergic pathway has also been implicated in social behaviors, suggesting a rewarding nature of social interactions (Gunaydin et al., 2014; Krach et al., 2010). The present study showed that SH mice exhibited deficits in social recognition without impairment of novel object recognition, indicating an a jSI-induced alteration in the mesolimbic dopaminergic pathway encompassing the IL-NAcSh circuit. Chronic social isolation in adult rats has been reported to decrease cAMP response element-binding protein (CREB) activity and the excitability of the NAcSh neurons: both effects may underlie depression-like behaviors in socially isolated rats (Wallace et al., 2009). We found that the excitability of NAcSh-projecting IL neurons is significantly decreased in SH mice, showing that the excitability of both mPFC and NAcSh neurons is affected by social isolation. Consistent with these observations, it has been shown that jSI reduces the excitability of a subtype of mPFC pyramidal neurons in layer 5 (Yamamuro et al., 2018). In addition, a recent study showed that 2 weeks of social isolation followed by 4 weeks of regrouping impairs social interaction and reduces the excitability of mPFC neurons projecting to the pPVT (Yamamuro et al., 2020). Altogether, these results suggest that neuronal subpopulations in the mPFC serve unique social functions (e.g., social interaction and recognition) by projecting to distinct subcortical areas. The molecular mechanism underlying reduced excitability in NAcSh-projecting IL neurons remains to be investigated. It would be interesting to examining the role of CREB in our jSI model.

Previous studies using jSI model reported that the first 2 weeks after weaning (postnatal day [PND] 21–35) is critical for the development of normal social preference (Bicks et al., 2020; Makinodan et al., 2012, 2017; Yamamuro et al., 2018). However, we found that this period was not long enough to induce long-lasting deficits in social recognition (Figures S2A–S2D). Piskorowski et al. (2016) showed that schizophrenia model mice (Df16(A)$^{+/-}$) exhibited defects in social recognition and that its related alterations of neuronal properties occurred only in their adult phase, after postnatal 5 weeks (PND 35), implying that the postnatal development of normal social recognition completes later than PND 35. Our data indicate that the critical period for social recognition is within postnatal 11 weeks. However, the impacts of social isolation and resocialization on social behaviors can be sensitive to experimental conditions, such as the duration of isolation/regrouping and the mode of resocialization (Liu et al., 2012; Makinodan et al., 2012, 2017).

The mPFC PL is also involved in social behaviors. Previous studies have shown that the PL plays critical roles in social preference via its connection to the NAc, amygdala, or striatum (Huang et al., 2020; Kim et al., 2017; Murugan et al., 2017). A previous study showed that the activation of PL neurons projecting to the core region of NAc diminishes social preference (Murugan et al., 2017). We also examined the role of the mPFC PL-NAcSh circuit in social behaviors and found that this circuit is involved in both social preference and recognition. Recently, however, Xing et al. (2021) reported that inactivation of NAcSh-projecting PL neurons impairs social recognition without affecting social preference; these findings conflict with our results. Although the reason for this discrepancy is not clear, different experimental conditions, including the dosage of CNO, might be responsible. Interestingly, the NAc reportedly has distinct inputs along its rostral-caudal axis (Reed et al., 2018). Hence, the targeting of different regions of the NAcSh may also have contributed to the inconsistency. Nevertheless, jSI selectively affected the excitability of NAcSh-projecting IL neurons, but not PL neurons.

Although the deficits in social preference or sociability have been extensively investigated in animal models of ASD, deficits in social recognition, such as a lack of differentiation between individuals, has often been reported in both ASD patients and animal models (Carter et al., 2011; Kanner, 1943; Kim et al., 2016; Molina et al., 2008). Our study highlights the importance of environmental effects on social recognition by showing that the IL-NAcSh circuit that encodes social familiarity is vulnerable to jSI. Our study thus advances understanding of not only the biological mechanism for social recognition but also the pathophysiology underlying social recognition impairments in ASD and related disorders.

STAR★METHODS

Detailed methods are provided in the online version of this paper and include the following:

- KEY RESOURCES TABLE
- RESOURCE AVAILABILITY
  - Lead contact

object $t_{44} = 4.573$, ****$p < 0.0001$. Two-way ANOVA with repeated measures: hM4Di group, n = 15 mice; interaction between treatment and social target, $F_{1,28} = 2.816$, $p = 0.1045$. Sidak's multiple comparison test: hM4Di Veh, mouse versus object $t_{44} = 11.29$, ****$p < 0.0001$; hM4Di CNO, mouse versus object $t_{44} = 13.9$, ****$p < 0.0001$. Right: social preference indices before and after CNO treatment were calculated from data shown in the middle panel. Two-tailed paired t test: mCherry, $p = 0.8871$; hM4Di, $p = 0.2551$.

(F) Left: representative heatmap image following the social recognition test. Middle: inactivation of IL-NAcSh neurons impairs social recognition. Two-way ANOVA with repeated measures: mCherry group, n = 12 mice; interaction between treatment and social target, $F_{1,22} = 1.239$, $p = 0.2776$. Sidak's multiple comparison test: mCherry Veh, S1 versus S2 $t_{44} = 5.965$, ****$p < 0.0001$; mCherry CNO, S1 versus S2 $t_{44} = 4.714$, ****$p < 0.0001$. Two-way ANOVA with repeated measures: hM4Di group, n = 15 mice; interaction between treatment and social target, $F_{1,28} = 12.39$, **$p = 0.0015$. Sidak's multiple comparison test: hM4Di Veh, S1 versus S2 $t_{56} = 5.276$, ****$p < 0.0001$; hM4Di CNO, S1 versus S2 $t_{56} = 0.2389$, $p = 0.9647$. Right: social preference indices before and after CNO treatment were calculated from data shown in the middle panel. Two-tailed paired t test: mCherry, $p = 0.4478$; hM4Di, *$p = 0.0260$.

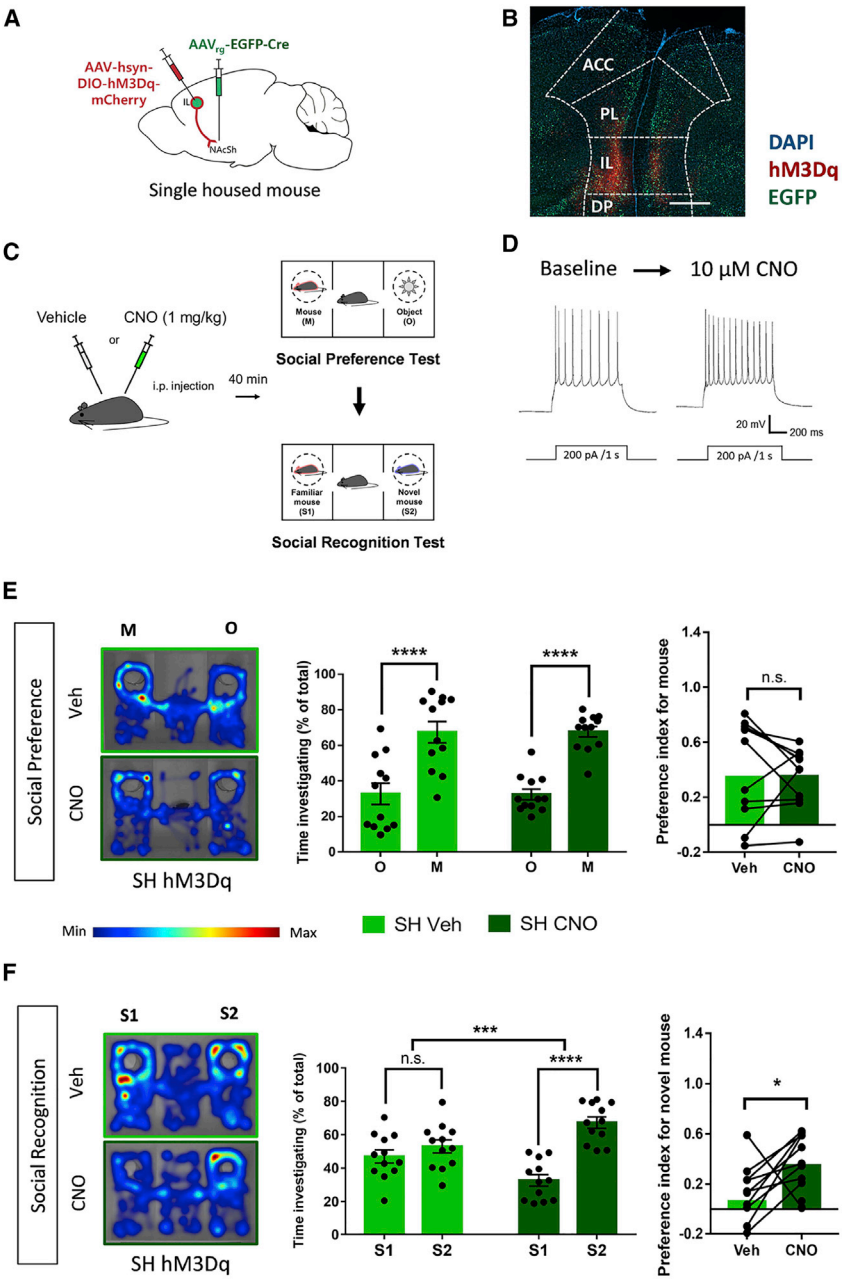

Figure 6. Chemogenetic activation of NAcSh-projecting IL neurons restores the social recognition deficit in SH mice

(A) Strategy of specifically expressing stimulatory G-protein (Gq)-coupled hM3Dq receptor in NAcSh-projecting IL neurons in SH mice.

(B) Representative image of mPFC expressing the hM3Dq receptor preferentially in IL neurons. Scale bar, 500 μm.

(C) Strategy of activating hM3Dq-expressing IL→NAcSh neurons during the 3-chamber social behavior tests by injecting CNO (1 mg/kg).

(D) Traces from the *ex vivo* whole-cell recording validated activation of the hM3Dq receptor with CNO treatment.

(E) Left: representative heatmap image of a CNO- or vehicle-injected hM3Dq-expressing SH mouse during the social preference test. Middle: activating IL-NAcSh neurons had no significant effect on social preferences in SH mice. n = 12 mice; interaction between treatment and target, $F_{1,22} = 0.005922$, p = 0.9394. Sidak's multiple comparison test: SH Veh $t_{44} = 5.19$, ****p < 0.0001; SH CNO $t_{44} = 5.284$, ****p < 0.0001. Right: CNO treatment did not affect the social preference index in SH mice. Two-tailed paired t test: p = 0.9528.

(F) Left: representative heatmap image for a CNO- or vehicle-injected hM3Dq-expressing SH mouse during the social recognition test. Middle: activation of IL-NAcSh neurons rescues the social recognition deficit in SH mice. Two-way ANOVA with repeated measures: n = 12 mice; interaction between treatment and social target, $F_{1,22} = 16.11$, ***p = 0.0006. Sidak's multiple comparison test: SH Veh $t_{44} = 1.178$, p = 0.4300; SH CNO $t_{44} = 6.668$, ****p < 0.0001. Right: CNO treatment significantly increases the social recognition index in SH mice. Two-tailed paired t test: *p = 0.0109.

SUPPLEMENTAL INFORMATION

Supplemental information can be found online at https://doi.org/10.1016/j.celrep.2021.109104.

ACKNOWLEDGMENTS

This work was supported by grants to Y.-S.L. (NRF-2017M3C7A1026959 and NRF-2019R1A4A2001609), S.J.K. (NRF-2018R1A5A2025964 and NRF-2017M3C7A1029611), and G.P. (NRF-2018H1A2A1061381) from the National Research Foundation of Korea. J.W.K. was supported by the KBRI basic research program (21-BR-02-06). The authors thank Han Byul Jang and Myeong Jong Yoo for helping with the management of the single-housing mouse colony.

AUTHOR CONTRIBUTIONS

G.P., C.R., J.W.K., S.J.K., and Y.-S.L. conceptualized the research and design the experiments. Y.-S.L. and S.J.K. supervised the research. G.P., C.R., and S.K. performed behavioral analyses. G.P., C.R., and S.J.J. performed whole-cell patch-clamp recordings and stereotaxic surgeries. G.P., C.R., J.W.K., and Y.-S.L. wrote and edited the manuscript.

DECLARATION OF INTERESTS

The authors declare no competing interests.

Received: October 10, 2020
Revised: February 26, 2021
Accepted: April 16, 2021
Published: May 11, 2021

REFERENCES

Albers, H.E. (2012). The regulation of social recognition, social communication and aggression: vasopressin in the social behavior neural network. Horm. Behav. *61*, 283–292.

Bicks, L.K., Koike, H., Akbarian, S., and Morishita, H. (2015). Prefrontal Cortex and Social Cognition in Mouse and Man. Front. Psychol. *6*, 1805.

Bicks, L.K., Yamamuro, K., Flanigan, M.E., Kim, J.M., Kato, D., Lucas, E.K., Koike, H., Peng, M.S., Brady, D.M., Chandrasekaran, S., et al. (2020). Prefrontal parvalbumin interneurons require juvenile social experience to establish adult social behavior. Nat. Commun. *11*, 1003.

Carter, M.D., Shah, C.R., Muller, C.L., Crawley, J.N., Carneiro, A.M.D., and Veenstra-VanderWeele, J. (2011). Absence of preference for social novelty and increased grooming in integrin β3 knockout mice: initial studies and future directions. Autism Res. *4*, 57–67.

Chisholm, K., Carter, M.C., Ames, E.W., and Morison, S.J. (1995). Attachment security and indiscriminately friendly behavior in children adopted from Romanian orphanages. Dev. Psychopathol. *7*, 283–294.

Chugani, H.T., Behen, M.E., Muzik, O., Juhász, C., Nagy, F., and Chugani, D.C. (2001). Local brain functional activity following early deprivation: a study of postinstitutionalized Romanian orphans. Neuroimage *14*, 1290–1301.

Corbit, L.H., Muir, J.L., and Balleine, B.W. (2001). The role of the nucleus accumbens in instrumental conditioning: Evidence of a functional dissociation between accumbens core and shell. J. Neurosci. *21*, 3251–3260.

Dang, T.P., Mattan, B.D., Kubota, J.T., and Cloutier, J. (2019). The ventromedial prefrontal cortex is particularly responsive to social evaluations requiring the use of person-knowledge. Sci. Rep. *9*, 5054.

Deng, X., Gu, L., Sui, N., Guo, J., and Liang, J. (2019). Parvalbumin interneuron in the ventral hippocampus functions as a discriminator in social memory. Proc. Natl. Acad. Sci. USA *116*, 16583–16592.

Donegan, M.L., Stefanini, F., Meira, T., Gordon, J.A., Fusi, S., and Siegelbaum, S.A. (2020). Coding of social novelty in the hippocampal CA2 region and its disruption and rescue in a 22q11.2 microdeletion mouse model. Nat. Neurosci. *23*, 1365–1375.

Eluvathingal, T.J., Chugani, H.T., Behen, M.E., Juhász, C., Muzik, O., Maqbool, M., Chugani, D.C., and Makki, M. (2006). Abnormal brain connectivity in children after early severe socioemotional deprivation: a diffusion tensor imaging study. Pediatrics *117*, 2093–2100.

Fukuda, H., Ma, N., Suzuki, S., Harasawa, N., Ueno, K., Gardner, J.L., Ichinohe, N., Haruno, M., Cheng, K., and Nakahara, H. (2019). Computing Social Value Conversion in the Human Brain. J. Neurosci. *39*, 5153–5172.

Fuster, J.M. (2002). Frontal lobe and cognitive development. J. Neurocytol. *31*, 373–385.

Gunaydin, L.A., Grosenick, L., Finkelstein, J.C., Kauvar, I.V., Fenno, L.E., Adhikari, A., Lammel, S., Mirzabekov, J.J., Airan, R.D., Zalocusky, K.A., et al. (2014). Natural neural projection dynamics underlying social behavior. Cell *157*, 1535–1551.

Hall, F.S. (1998). Social deprivation of neonatal, adolescent, and adult rats has distinct neurochemical and behavioral consequences. Crit. Rev. Neurobiol. *12*, 129–162.

Hitti, F.L., and Siegelbaum, S.A. (2014). The hippocampal CA2 region is essential for social memory. Nature *508*, 88–92.

Huang, W.-C., Zucca, A., Levy, J., and Page, D.T. (2020). Social Behavior Is Modulated by Valence-Encoding mPFC-Amygdala Sub-circuitry. Cell Rep. *32*, 107899.

Kanner, L. (1943). Autistic disturbances of affective contact. Nerv. Child *2*, 217–250.

Kim, Y., Venkataraju, K.U., Pradhan, K., Mende, C., Taranda, J., Turaga, S.C., Arganda-Carreras, I., Ng, L., Hawrylycz, M.J., Rockland, K.S., et al. (2015). Mapping social behavior-induced brain activation at cellular resolution in the mouse. Cell Rep. *10*, 292–305.

Kim, S., Kim, T., Lee, H.-R., Jang, E.-H., Ryu, H.-H., Kang, M., Rah, S.-Y., Yoo, J., Lee, B., Kim, J.-I., et al. (2016). Impaired learning and memory in CD38 null mutant mice. Mol. Brain *9*, 16.

Kim, H., Lee, Y., Park, J.Y., Kim, J.E., Kim, T.K., Choi, J., Lee, J.E., Lee, E.H., Kim, D., Kim, K.S., and Han, P.L. (2017). Loss of Adenylyl Cyclase Type-5 in the Dorsal Striatum Produces Autistic-Like Behaviors. Mol. Neurobiol. *54*, 7994–8008.

Kim, D.-Y., Heo, G., Kim, M., Kim, H., Jin, J.A., Kim, H.-K., Jung, S., An, M., Ahn, B.H., Park, J.H., et al. (2020). A neural circuit mechanism for mechanosensory feedback control of ingestion. Nature *580*, 376–380.

Klawonn, A.M., and Malenka, R.C. (2018). Nucleus Accumbens Modulation in Reward and Aversion. Cold Spring Harb. Symp. Quant. Biol. *83*, 119–129.

Kohls, G., Perino, M.T., Taylor, J.M., Madva, E.N., Cayless, S.J., Troiani, V., Price, E., Faja, S., Herrington, J.D., and Schultz, R.T. (2013). The nucleus accumbens is involved in both the pursuit of social reward and the avoidance of social punishment. Neuropsychologia *51*, 2062–2069.

Krach, S., Paulus, F.M., Bodden, M., and Kircher, T. (2010). The rewarding nature of social interactions. Front. Behav. Neurosci. *4*, 22.

Kreppner, J.M., O'Connor, T.G., Dunn, J., and Andersen-Wood, L.; English and Romanian Adoptees (ERA) Study Team (1999). The pretend and social role play of children exposed to early severe deprivation. Br. J. Dev. Psychol. *17*, 319–332.

Krishnan, V., Han, M.-H., Graham, D.L., Berton, O., Renthal, W., Russo, S.J., Laplant, Q., Graham, A., Lutter, M., Lagace, D.C., et al. (2007). Molecular adaptations underlying susceptibility and resistance to social defeat in brain reward regions. Cell *131*, 391–404.

Lafferty, C.K., Yang, A.K., Mendoza, J.A., and Britt, J.P. (2020). Nucleus Accumbens Cell Type- and Input-Specific Suppression of Unproductive Reward Seeking. Cell Rep. *30*, 3729–3742.e3.

Layden, E.A., Cacioppo, J.T., Cacioppo, S., Cappa, S.F., Dodich, A., Falini, A., and Canessa, N. (2017). Perceived social isolation is associated with altered functional connectivity in neural networks associated with tonic alertness and executive control. Neuroimage *145* (*Pt A*), 58–73.

Lee, J., Finkelstein, J., Choi, J.Y., and Witten, I.B. (2016). Linking Cholinergic Interneurons, Synaptic Plasticity, and Behavior during the Extinction of a Cocaine-Context Association. Neuron *90*, 1071–1085.

Lerner, T.N., et al. (2015). Intact-Brain Analyses Reveal Distinct Information Carried by SNc Dopamine Subcircuits. Cell *162*, 635–647.

Li, Z., Chen, Z., Fan, G., Li, A., Yuan, J., and Xu, T. (2018). Cell-Type-Specific Afferent Innervation of the Nucleus Accumbens Core and Shell. Front. Neuroanat. *12*, 84.

Liu, X., and Carter, A.G. (2018). Ventral Hippocampal Inputs Preferentially Drive Corticocortical Neurons in the Infralimbic Prefrontal Cortex. J. Neurosci. *38*, 7351–7363.

Liu, J., Dietz, K., DeLoyht, J.M., Pedre, X., Kelkar, D., Kaur, J., Vialou, V., Lobo, M.K., Dietz, D.M., Nestler, E.J., et al. (2012). Impaired adult myelination in the prefrontal cortex of socially isolated mice. Nat. Neurosci. *15*, 1621–1623.

Loureiro, M., Achargui, R., Flakowski, J., Van Zessen, R., Stefanelli, T., Pascoli, V., and Lüscher, C. (2019). Social transmission of food safety depends on synaptic plasticity in the prefrontal cortex. Science *364*, 991–995.

Lu, D.-H., Liao, H.-M., Chen, C.-H., Tu, H.-J., Liou, H.-C., Gau, S.S.-F., and Fu, W.-M. (2018). Impairment of social behaviors in *Arhgef10* knockout mice. Mol. Autism *9*, 11.

Makinodan, M., Rosen, K.M., Ito, S., and Corfas, G. (2012). A critical period for social experience-dependent oligodendrocyte maturation and myelination. Science *337*, 1357–1360.

Makinodan, M., Ikawa, D., Yamamuro, K., Yamashita, Y., Toritsuka, M., Kimoto, S., Yamauchi, T., Okumura, K., Komori, T., Fukami, S.-I., et al. (2017). Effects of the mode of re-socialization after juvenile social isolation on medial prefrontal cortex myelination and function. Sci. Rep. *7*, 5481.

McKibben, C.E., Reynolds, G.P., and Jenkins, T.A. (2014). Analysis of sociability and preference for social novelty in the acute and subchronic phencyclidine rat. J. Psychopharmacol. *28*, 955–963.

Medendorp, W.E., Petersen, E.D., Pal, A., Wagner, L.-M., Myers, A.R., Hochgeschwender, U., and Jenrow, K.A. (2018). Altered Behavior in Mice Socially Isolated During Adolescence Corresponds With Immature Dendritic Spine Morphology and Impaired Plasticity in the Prefrontal Cortex. Front. Behav. Neurosci. *12*, 87.

Meira, T., Leroy, F., Buss, E.W., Oliva, A., Park, J., and Siegelbaum, S.A. (2018). A hippocampal circuit linking dorsal CA2 to ventral CA1 critical for social memory dynamics. Nat. Commun. *9*, 4163.

Molina, J., Carmona-Mora, P., Chrast, J., Krall, P.M., Canales, C.P., Lupski, J.R., Reymond, A., and Walz, K. (2008). Abnormal social behaviors and altered gene expression rates in a mouse model for Potocki-Lupski syndrome. Hum. Mol. Genet. *17*, 2486–2495.

Moy, S.S., Nadler, J.J., Perez, A., Barbaro, R.P., Johns, J.M., Magnuson, T.R., Piven, J., and Crawley, J.N. (2004). Sociability and preference for social novelty in five inbred strains: an approach to assess autistic-like behavior in mice. Genes Brain Behav. *3*, 287–302.

Murugan, M., Jang, H.J., Park, M., Miller, E.M., Cox, J., Taliaferro, J.P., Parker, N.F., Bhave, V., Hur, H., Liang, Y., et al. (2017). Combined Social and Spatial Coding in a Descending Projection from the Prefrontal Cortex. Cell *171*, 1663–1677.

Numa, C., Nagai, H., Taniguchi, M., Nagai, M., Shinohara, R., and Furuyashiki, T. (2019). Social defeat stress-specific increase in c-Fos expression in the extended amygdala in mice: Involvement of dopamine D1 receptor in the medial prefrontal cortex. Sci. Rep. *9*, 16670.

Okuyama, T., Kitamura, T., Roy, D.S., Itohara, S., and Tonegawa, S. (2016). Ventral CA1 neurons store social memory. Science *353*, 1536–1541.

Piskorowski, R.A., Nasrallah, K., Diamantopoulou, A., Mukai, J., Hassan, S.I., Siegelbaum, S.A., Gogos, J.A., and Chevaleyre, V. (2016). Age-Dependent Specific Changes in Area CA2 of the Hippocampus and Social Memory Deficit in a Mouse Model of the 22q11.2 Deletion Syndrome. Neuron *89*, 163–176.

Porsolt, R.D., Le Pichon, M., and Jalfre, M. (1977). Depression: a new animal model sensitive to antidepressant treatments. Nature *266*, 730–732.

Reed, S.J., Lafferty, C.K., Mendoza, J.A., Yang, A.K., Davidson, T.J., Grosenick, L., Deisseroth, K., and Britt, J.P. (2018). Coordinated Reductions in Excitatory Input to the Nucleus Accumbens Underlie Food Consumption. Neuron *99*, 1260–1273.e4.

Rutter, M., Andersen-Wood, L., Beckett, C., Bredenkamp, D., Castle, J., Groothues, C., Kreppner, J., Keaveney, L., Lord, C., and O'Connor, T.G.; English and Romanian Adoptees (ERA) Study Team (1999). Quasi-autistic patterns following severe early global privation. J. Child Psychol. Psychiatry *40*, 537–549.

Rutter, M., Kreppner, J., Croft, C., Murin, M., Colvert, E., Beckett, C., Castle, J., and Sonuga-Barke, E. (2007). Early adolescent outcomes of institutionally deprived and non-deprived adoptees. III. Quasi-autism. J. Child Psychol. Psychiatry *48*, 1200–1207.

Ryu, C., Jang, D.C., Jung, D., Kim, Y.G., Shim, H.G., Ryu, H.-H., Lee, Y.-S., Linden, D.J., Worley, P.F., and Kim, S.J. (2017). STIM1 Regulates Somatic Ca^{2+} Signals and Intrinsic Firing Properties of Cerebellar Purkinje Neurons. J. Neurosci. *37*, 8876–8894.

Squire, L.R., and Zola-Morgan, S. (1991). The medial temporal lobe memory system. Science *253*, 1380–1386.

Tanimizu, T., Kenney, J.W., Okano, E., Kadoma, K., Frankland, P.W., and Kida, S. (2017). Functional Connectivity of Multiple Brain Regions Required for the Consolidation of Social Recognition Memory. J. Neurosci. *37*, 4103–4116.

Tzakis, N., and Holahan, M.R. (2019). Social Memory and the Role of the Hippocampal CA2 Region. Front. Behav. Neurosci. *13*, 233.

Wagner, D.D., Kelley, W.M., Haxby, J.V., and Heatherton, T.F. (2016). The Dorsal Medial Prefrontal Cortex Responds Preferentially to Social Interactions during Natural Viewing. J. Neurosci. *36*, 6917–6925.

Wallace, D.L., Han, M.-H., Graham, D.L., Green, T.A., Vialou, V., Iñiguez, S.D., Cao, J.-L., Kirk, A., Chakravarty, S., Kumar, A., et al. (2009). CREB regulation of nucleus accumbens excitability mediates social isolation-induced behavioral deficits. Nat. Neurosci. *12*, 200–209.

Wang, N., Ge, F., Cui, C., Li, Y., Sun, X., Sun, L., Wang, X., Liu, S., Zhang, H., Liu, Y., et al. (2018). Role of Glutamatergic Projections from the Ventral CA1 to Infralimbic Cortex in Context-Induced Reinstatement of Heroin Seeking. Neuropsychopharmacology *43*, 1373–1384.

Webb, S.J., Jones, E.J.H., Merkle, K., Namkung, J., Toth, K., Greenson, J., Murias, M., and Dawson, G. (2010). Toddlers with elevated autism symptoms show slowed habituation to faces. Child Neuropsychol. *16*, 255–278.

Weiss, I.C., Pryce, C.R., Jongen-Rêlo, A.L., Nanz-Bahr, N.I., and Feldon, J. (2004). Effect of social isolation on stress-related behavioural and neuroendocrine state in the rat. Behav. Brain Res. *152*, 279–295.

Xing, B., Mack, N.R., Guo, K.-M., Zhang, Y.-X., Ramirez, B., Yang, S.-S., Lin, L., Wang, D.V., Li, Y.-C., and Gao, W.-J. (2021). A Subpopulation of Prefrontal Cortical Neurons Is Required for Social Memory. Biol. Psychiatry *89*, 521–531.

Xu, P., He, Y., Cao, X., Valencia-Torres, L., Yan, X., Saito, K., Wang, C., Yang, Y., Hinton, A., Jr., Zhu, L., et al. (2017). Activation of Serotonin 2C Receptors in Dopamine Neurons Inhibits Binge-like Eating in Mice. Biol. Psychiatry *81*, 737–747.

Yamamuro, K., Yoshino, H., Ogawa, Y., Makinodan, M., Toritsuka, M., Yamashita, M., Corfas, G., and Kishimoto, T. (2018). Social Isolation During the Critical Period Reduces Synaptic and Intrinsic Excitability of a Subtype of Pyramidal Cell in Mouse Prefrontal Cortex. Cereb. Cortex *28*, 998–1010.

Yamamuro, K., Bicks, L.K., Leventhal, M.B., Kato, D., Im, S., Flanigan, M.E., Garkun, Y., Norman, K.J., Caro, K., Sadahiro, M., et al. (2020). A prefrontal-paraventricular thalamus circuit requires juvenile social experience to regulate adult sociability in mice. Nat. Neurosci. *23*, 1240–1252.

Yizhar, O., Fenno, L.E., Prigge, M., Schneider, F., Davidson, T.J., O'Shea, D.J., Sohal, V.S., Goshen, I., Finkelstein, J., Paz, J.T., et al. (2011). Neocortical excitation/inhibition balance in information processing and social dysfunction. Nature *477*, 171–178.

Young, L.J. (2002). The neurobiology of social recognition, approach, and avoidance. Biol. Psychiatry *51*, 18–26.

STAR★METHODS

KEY RESOURCES TABLE

REAGENT or RESOURCE	SOURCE	IDENTIFIER
Antibodies		
Rabbit monoclonal anti-c-Fos (9F6)	Cell Signaling Technology	Cat#2250; RRID: AB_2247211
Alexa fluor 594-conjugated donkey anti-rabbit IgG	Invitrogen	Cat#A-21207; RRID: AB_141637
Bacterial and virus strains		
AAVrg-Ef1a-mCherry-IRES-Cre	Addgene	Cat#55632-AAVrg; Plasmid RRID: Addgene_55632
AAVrg-hsyn-HI-eGFP-Cre	Addgene	Cat#105540-AAVrg; Plasmid RRID: Addgene_105540
AAV-DIO-hM4D(Gi)-mCherry	Addgene	Cat#44362-PHPeB; Plasmid RRID: Addgene_44362
AAV-DIO-hM3D(Gq)-mCherry	Addgene	Cat#44361-PHPeB; Plasmid RRID: Addgene_44361
AAV-DIO-mCherry	Addgene	Cat#50459-AAV9; Plasmid RRID: Addgene_50459
AAV-Flex-GCaMP6s	Addgene	Cat#100845-AAV5; Plasmid RRID: Addgene_100845
Chemicals, peptides, and recombinant proteins		
Normal Donkey Serum	Sigma	Cat#D9663
Triton X-100	Sigma	Cat#x100
DAPI	Thermo Scientific™	Cat#62248
Mounting Solution	Vector	Cat#H-1000
Zoletil	Virbac	N/A
Xylazine	Bayer	N/A
Experimental models: Organisms/strains		
C57BL/6NHsd	Koatech	N/A
C57BL/6NCrljOri	Orient Bio	N/A
Software and algorithms		
Zen	Zeiss	RRID: SCR_013672
Ethovision XT 11.5	Noldus	RRID: SCR_000441
Python 3.7	Python	http://www.python.org
GraphPad Prism	GraphPad	RRID:SCR_002798
Patchmaster	HEKA	RRID:SCR_000034
Synapse	Tucker-Davis Technologies	N/A
Minhee Analysis	Labview	https://github.com/parkgilbong/Minhee_Analysis_Pack
IntrinsicVIEW	Labview	https://github.com/parkgilbong/IntrinsicVIEW
Other		
Side Scanner ZEISS Axio Scan.Z1	ZEISS	N/A
Nanoliter 2010 Injector	WPI	N/A
Python code for fiber photometry analysis (Lerner, 2015)	Tucker-Davis Technologies	https://www.tdt.com/support/python-sdk/

RESOURCE AVAILABILITY

Lead contact

Further information and requestions for resources and reagents should be directed to and will be fulfilled by the Lead Contact, Yong-Seok Lee (yongseok7@snu.ac.kr).

Materials availability

This study did not generate new unique reagents.

Data and code availability

All software or algorithm used in this study is available and listed in the Key Resources Table. The data that support the findings of this study are available upon reasonable request from the lead contact.

EXPERIMENTAL MODEL AND SUBJECT DETAILS

Male C57BL/6NHsd mice were purchased from Koatech (South Korea). Purchased mice were introduced to the animal facility at Seoul National University College of Medicine on postnatal day 14 (PND14) with their dam. Four mice were allocated into a standard mouse cage with their dam. At PND 21, mice were weaned from their dam. From PND 70 to PND 90, the mice may experience the surgical procedure depending on the experimental needs. Social conspecifics C57BL/6NCrljOri were purchased by another breeder in Korea (Orient Bio) at PND 35 and used for the social behavior test after an adjustment period of 1 week. All mice were given by a fixed 12 hours light-dark cycle (light on: 8:00-20:00; light off: 20:00 – next day 8:00). Food and water were provided *ad libitum*. Experiments were conducted in accordance with the Seoul National University, College of Medicine, Department of Physiology and approved by the Institutional Animal Care and Use Committee of Seoul National University (IACUC #: SNU 190501-5-2).

METHOD DETAILS

Social isolation

At PND 21, group-housed (GH) mice were removed from their dam, but still housed with their littermates. Single-housed (SH) mice were individually housed in the standard mouse cage from PND 21 to PND 77 (isolated for 8 weeks) or from PND 21 to PND 35 (for 2 weeks). After 8 weeks of isolation, single-isolated mice were re-grouped with their littermates.

Surgical procedures

Mice were anesthetized with a Zoletil (30 mg/kg) and Rompun (10 mg/kg) mixture prior to the surgical procedure by i.p. injection with the injection volume varying depend on body weight. The anesthetized mouse was set on the rodent stereotaxic apparatus. A heating pad was placed below the mouse to prevent rodent hypothermia during the stereotaxic surgery. An appropriate region of the skull was drilled with a stereotaxically fastened hand drill assembled with a 0.4 mm drill bit. Virus injection was performed bilaterally. The infralimbic cortex (AP +2.4 from bregma, ML ± 1.0 from midline, DV −2.3 from skull; 10° angle given to avoid virus expression in the prelimbic cortex) and nucleus accumbens shell (AP +1.94 from bregma, ML ± 0.55 from midline, DV −4.15 from skull) were targeted for virus injection. A glass capillary (#504949, WPI, USA) is pulled out sharply using the Dual-Stage Glass Micropipette Puller (NARISHIGE, USA). For retrograde tracing and labeling, AAVrg-Ef1a-mCherry-IRES-Cre or AAVrg-hsyn-HI-eGFP-Cre was injected as 5×10^{12} GC/mL (500 nL) or 7.5×10^{12} GC/mL (150 nL) into the NAcSh. For chemogenetic manipulation, AAV-DIO-hM4Di-mCherry, AAV-DIO-hM3Dq-mCherry, or AAV-DIO- mCherry was injected as 7.5×10^{12} GC/mL (150 nL) into the IL together with Cre virus into the NAcSh. For fiber photometry recording, AAV-Flex-GCaMP6s was injected as 7.5×10^{12} GC/mL (150 nL) into the IL together with Cre virus into the NAcSh. The virus was diluted with filtered ACSF to the desired titer. Nanoliter 2010 (WPI) or Spritzer Pressure System IIe (Toohey Company, USA) was used for the virus injection. The virus was given toward the target of interest with a speed of 20 μL/min, giving the desired volume of virus depending on the experiment and brain regions. The capillary was set still within the brain at least 5 min before a slow withdrawal. The glass capillary was pulled off slowly and the incised skin was sutured with sterilized suture thread. Animals were rested at least 3 weeks before further experiments.

CNO administration

To activate designer receptors exclusively activated by designer drugs (DREADD), we used clozapine N-oxide (CNO) dihydrochloride (water soluble form, Hello Bio) dissolved in 0.9% normal saline to yield a final concentration of 1 mg/mL. CNO solution (final concentration in the body: 3 mg/kg for hM4Di neuronal inhibition; 1 mg/kg for hM3Dq neuronal activation) or the same volume of saline vehicle was i.p. injected into mice 40 minutes before behavioral assessments (Xu et al., 2017). In hM4Di experiments, CNO or vehicle injection into each mouse was separated by 2 days and the order of injections was counterbalanced: If the first behavioral test was conducted after the injection of the CNO; two days later, the mice were injected with vehicle and then subjected to the second behavioral test or vice versa. In hM3Dq experiments, the mice were always injected with vehicle and two days later they were injected with CNO.

Behavior Tests

All behavior tests described below were performed in a soundproof chamber with a dim light illumination during the light-on cycle. All behavior tests were recorded by the camcorder and the experimenters were blinded to the experimental conditions. Both the subject and target mice were habituated for hand approach made by a human prior to any behavior test. Mice behavior was recorded using a mouse-tracking software (EthoVision XT 11.5, Noldus, Netherlands) and followed by manual scoring for mice interaction time as describe below.

Three-chamber social behavior test

The three-chamber social behavior test was performed as previously described (Moy et al., 2004). We used a white opaque acrylic three-chambered apparatuses with two doors between the chambers (40 × 60 cm size, each chamber 20-cm wide). Before the test, target mice were habituated in wire containers placed in side-chambers in the apparatuses for 20 minutes on 2 consecutive days. Each subject mouse was placed in a test consisting of three sessions: (1) habituation, (2) social preference test, (3) social recognition test. For the habituation, the subject mouse was put in the apparatus for 10 minutes with the doors open. After the habituation, the social preference test was performed. The first target mouse was put in a wire container in either the left or right chamber. An inanimate object (mouse-shaped plastic toy) was put in the wire cage in the other side chamber. For the social recognition test, an inanimate object was replaced by another target mouse. During the intervals between sessions, the subject mouse was gently guided to the center room of the apparatus and the doors of the apparatus were closed. After the placement of target mice, the doors were re-opened, and the subject mouse was re-allowed to move freely for 10 minutes. The movements of subject mice during the test were tracked by a mouse tracking software (EthoVision XT 11.5, Noldus). Interaction times with conspecifics were manually scored by researchers who were blinded to the mouse groupings. The time that the mice spent sniffing the wired cup or body parts such as the tail or toe was considered as interaction time. The identity of mice was disclosed to the researchers after the manual scoring was completed. To normalize the variation in the exploration time of each subject, all data were represented by the percentage of time spent investigating one side out of total investigation time for both sides. However, real time interaction time (in sec) has been shown in the Supplemental information. Total exploration time has been obtained from the summation of exploration time in two targets (mouse and object or familiar mouse and novel mouse). Preference index (PI) was calculated by following equations (ET_M: exploration time for a mouse; ET_O: exploration time for an object; ET_N: exploration time for a novel mouse (the second target mouse); ET_F: exploration time for a familiar mouse (the first target mouse)).

$$PI\ for\ social\ preference\ = \frac{ET_M - ET_0}{ET_M + ET_0}$$

$$PI\ for\ social\ recognition\ = \frac{ET_N - ET_F}{ET_N + ET_F}$$

Reciprocal social interaction test

A clean mouse homecage with a thin layer of bedding was used for the reciprocal social interaction test. Two mice (either two subject mice or one subject mouse and a target mouse) were placed in the homecage simultaneously. Mouse interaction was recorded and manually analyzed. For the interaction, nose-to-nose and nose-to-anogenital sniffing times were counted.

Social habituation/recognition task

Subject mice were allocated to the home cage individually at one hour before the behavior test. Subject mice were placed in a white opaque acrylic box (33 × 33 cm size box) with the wired cup. The social habituation/recognition test was comprised of three sessions: (1) habituation, (2) familiarization, and (3) retrieval. The social habituation/recognition task took 2 days; habituation and familiarization were performed on day 1, and interaction was tested on day 2. The habituation session allowed mice to explore the while opaque acrylic box with a wired cup for 10 minutes. The target conspecific was introduced into the wired container for 5 minutes. This familiarization was repeated twice more with a 90-minute interval. Subject mice were returned to their individual home cages after familiarization. On day 2, the subject mice were exposed to the same environment to the familiarization. However, the subject mice randomly explored the wired cup that was either filled with a novel conspecific, a familiar conspecific, or nothing.

Open field test

Subject mice were placed in the center of a white opaque acrylic box (33 × 33 cm size) to move freely for 10 minutes. The center zone was set in 20 × 20 cm size. The movements of subject mice were tracked by EthoVision XT 11.5 (Noldus).

Novel object recognition test

Prior to the test, subject mice were habituated to a test arena (33 × 33 cm size, white opaque acrylic box) for 20 minutes on 2 consecutive days. On the day of the test, training and test sessions were conducted. For the training session, the subject mouse was put in the center of the test arena containing two identical objects (pair #1). The mouse was allowed to move freely for 10 minutes. After the training session, the mouse was taken out from the test arena, and one of the objects was replaced with a novel object (pair #2). To avoid providing any scent cue toward the subject mice, the original object placed inside the test arena was wiped with 70% ethanol. Immediately after the object replacement and brief cleaning, the mouse was reintroduced into the test arena to move freely for 10 minutes. In the DREADD experiments, different pairs of objects were used when the mice were injected with CNO or vehicle to avoid any redundancy. Hence, four different pairs of objects were used in the DREADD experiment for each subject mouse. The time that the

mouse spent investigating the object was manually counted as the time spent close enough to the object that allowed for sniffing. To normalize the variation in the exploration time of each subject, all data were represented by the percentage of time spent investigating one side out of the total investigation time for both sides.

Object place recognition test

Prior to the test, subject mice were habituated to a test arena (33 × 33 cm size, white opaque acrylic box) for 10 minutes twice on the same day. On the day of the test, training and test sessions were conducted. For the training session, the subject mouse was put in the center of the test arena containing two identical objects. To give a spatial cue to the subject mice, a triangle was put on one side of the box. The mouse was allowed to move freely for 10 minutes. After the training session, the mouse was taken out from the test arena, and one of the objects was moved vertically to a novel location. Then, the mouse was reintroduced into the test arena to move freely for 10 minutes. Two different pairs of objects were used in the DREADD experiments for each subject mouse. To normalize the variation in the exploration time of each subject, all data were represented by the percentage of time spent investigating one side out of the total investigation time for both sides.

Elevated plus maze test

The apparatus consisted of two open arms (29.5 × 5 x 0.5 cm), two perpendicular closed arms (29.5 × 5 x 16 cm), and a center platform (5 × 5 x 0.5 cm). The apparatus was raised 50 cm above the floor. The open arms had a short wall (0.5 cm) to keep animals from falling or escaping, whereas the closed arms had a tall wall (16 cm). The subject mouse was placed in the center of the apparatus (with its head heading toward open arms) and was allowed to move freely for 10 minutes. The exploration time to each arm was scored using EthoVision XT 11.5 (Noldus).

Immunohistochemistry

Brains of the subject mice were extracted after carrying out transcardial perfusion by PBS solution followed by 4% PFA solution (T&I, Korea). Perfused brains were emerged into 4% PFA for 24 hours and emerged into 30% (w/v) sucrose solution for 48 hours. Processed brains were frozen at −20°C with clear frozen section compound (FSC22; Leica, Germany) and sliced at a 30 μm thickness. Brain slices were stored in CPS solution for the next usage. Brain slices were incubated with 4% (v/v) goat serum in 0.1% (v/v) Triton X-100 in PBS for 40 min. Brain slices were then incubated with primary antibodies primary antibodies [Anti-c-Fos (9F6), Cell signaling #2250] above a locker at 4°C for 48 hours. After 48 hr, brain slices were incubated with an appropriate secondary antibody (Alexa fluor 594-conjugated donkey anti-rabbit IgG, A-21207, Invitrogen) on room temperature for 4 hours. Before mounting the slices, DAPI (Cat #62248; Thermo Scientific, USA; 1:10,000) was added for counterstaining. Images were acquired using a confocal microscope FV3000 (Olympus) or Axio Scan Z1 (Zeiss). The fluorescent labeled cells in four to five brain slices from each mouse were were counted and averaged.

Electrophysiology

Electrophysiological recordings were performed as described previously (Ryu et al., 2017). Coronal slices of the mPFC (300 μm thick) were obtained by a vibratome (VT1200s, Leica) after isoflurane anesthesia and decapitation. Slices were cut in ice-cold cutting solution containing (in mM): 93 N-Methyl-D-glucamine (NMDG), 2.5 KCl, 10 $MgSO_4$, 0.5 $CaCl_2$, 1.25 NaH_2PO_4, 30 $NaHCO_3$, 25 glucose, 10 HEPES, 5 Na ascorbate, 2 thiourea, 3 Na pyruvate, 12 L- acetyl - cysteine, perfused with 95% O_2 and 5% CO_2. The slices immediately transferred to the same cutting solution at 32°C for 10 minutes, and then transferred to artificial cerebrospinal fluid (ACSF) at room temperature containing (in mM): 125 NaCl, 2.5 KCl, 1 $MgCl_2$, 2 $CaCl_2$, 1.25 NaH_2PO_4, 26 $NaHCO_3$, 10 glucose, perfused with 95% O_2 and 5% CO_2. The slices were recovered in ACSF for 1 hour before the experiment. All recordings were done within 8 hours from recovery. Brain slices were placed in a submerged chamber and perfused with ACSF for at least 10 minutes before recording. All recordings were made at 32°C. We used recording pipettes (4-5MΩ) filled with (in mM): 135 K-gluconate, 5 KCl, 2 NaCl, 10 HEPES, 0.1 EGTA, 5 Mg ATP, 0.4 Na_3 GTP and 10 Tris(di) phosphocreatine (pH 7.20 adjusted by KOH). Data were acquired using an EPC-9 patch-clamp amplifier (HEKA Elektronik) and PatchMaster software (HEKA Elektronik) with a 20 kHz sampling rate, and the signals were filtered at 2 kHz. Synaptic current data were analyzed using Mini Analysis (Synaptosoft). Excitability data were analyzed by customized LabView (National Instruments) analysis programs (https://github.com/parkgilbong/Minhee_Analysis_Pack).

Fiber photometry recording

Fiber photometry experiments were performed as previously described (Kim et al., 2020). Briefly, retrograde mCherry-cre virus was bilaterally injected into the NAcSh, and Flex-GCaMP6s virus was unilaterally injected into the infralimbic cortex. For the recording, a 400 μm core fiber optic cannula (RWD, R-FOC-L400C, 0.5NA) was implanted at 2.2 mm below the skull at an angle of 10° to prevent any damage in PL. The fiber optic cannula was fixed to the skull with vetbond and dental cement. Excitation lights from 465 nm and 405 nm LED (Doric Lenses) were modulated sinusoidally by a TDT fiber photometry real-time processor (RZ5P, Tucker Davis Technologies) at 211 Hz and 531 Hz, respectively. The light intensity was maintained at 0.1-0.2 mW during mouse behavior. The resulting signals were demodulated, amplified, and collected at around 1 kHz with both the TDT RZ5P processor and Synapse software (Tucker Davis Technologies). Mice behavior was recorded with a camcorder during the performance of fiber photometry. Obtained fiber photometry data was processed with python codes provided by TDT. For each mouse, 5 to 11 non-sequential social interaction

events with familiar conspecifics and 7 to 15 social interaction events with novel conspecific were used for the analysis. Non-sequential social interaction was sorted for the event that had a time gap of more than 10 s from the end of the previous social event. During social behavior tests, baseline was defined as a period of 2 s beginning from10 s before the interaction initiation (Yamamuro et al., 2020). The Z-score for −8 s to 10 s from interaction onset for each event was calculated using the average and standard deviation of the baseline dF/F.

QUANTIFICATION AND STATISTICAL ANALYSIS

A two-way repeated-measure analysis of variance (ANOVA) was performed was followed by an appropriate multiple comparisons post-test to analyze membrane excitability data, social preference, social recognition, object recognition, and object place recognition test. Preference indices and other two-group data were compared using an unpaired or paired two-tailed t test. Four-group data were compared using one-way ANOVA. All data are represented as the mean ± SEM. Graphpad prism 7.0 (Graphpad software) was used for all the statistical analyses and visualization.